# REPORT DOCUMENTATION PAGE

AFRL-SR-BL-TR-00-

0543



| 1. AGENCY USE ONLY (Leave blank) | 2. REPORT DATE | 3. REPORT TYPE AND DATES COVERED |
|---|---|---|
| | 20 July 2000 | Final Technical Report (30 Sep 1999 – 30 Jun 2000) |

**4. TITLE AND SUBTITLE**
Wavelet Based Analysis and Software for Multi-Scale Fractal Processes

**5. FUNDING NUMBERS**
C: FQ8671-9901279

**6. AUTHOR(S)**
Dr. William Constantine
Dr. Donald Percival

**7. PERFORMING ORGANIZATION NAME(S) AND ADDRESS(ES)**
MathSoft, Inc.
1700 Westlake Avenue North
Suite 500
Seattle, WA 98109-3044
USA

**8. PERFORMING ORGANIZATION REPORT NUMBER**
RES 160 0001AE

**9. SPONSORING / MONITORING AGENCY NAME(S) AND ADDRESS(ES)**

Sponsor:
USAF, AFMC
Air Force Office of Scientific Research
801 Randolph St, Room 732
Arlington, VA 22203-1977

Program Manager:
Air Force Office of Scientific Research
AFOSR/NX ATTN: Dr. Arje Nachman
801 North Randolph Street, Room 732
Arlington, VA 22203-1977

**10. SPONSORING / MONITORING AGENCY REPORT NUMBER**
0001AE

**11. SUPPLEMENTARY NOTES**



**12a. DISTRIBUTION / AVAILABILITY STATEMENT**
Approved for public release; distribution unlimited.

**12b. DISTRIBUTION CODE**

**13. ABSTRACT** *(Maximum 200 Words)*

Report developed under STTR contract for topic AF99T004. In this final technical report, we summarize the technical objectives, work accomplished, results, and technical feasibility. The primary objective of this research is to develop methodology and software for the analysis of atmospheric turbulence and related data. Turbulence data are challenging because they are inherently non-stationary across a range of scales. Because the discrete wavelet transform is a natural tool for use with non-stationary and scale-dependent data, we investigate the efficacy of a variety of wavelet-based techniques including approximate maximum likelihood and least squares estimators of power-law processes. These estimators are adapted to work effectively in the presence of (i) slow variations in the power-law parameters, (ii) large-scale stochastic trends and (iii) small-scale non-turbulent events. We examine the statistical properties of (most) wavelet-based power-law parameter estimators and develop corresponding confidence intervals. We also assess the efficacy of nonlinear deterministic models for turbulence data. All software was implemented in MathSoft's next generation S+WAVELETS module.

**14. SUBJECT TERMS**
turbulence; wavelet; STTR Report; fractal; subband modeling; prediction; stochastic; deterministic

**15. NUMBER OF PAGES**
26

**16. PRICE CODE**

| 17. SECURITY CLASSIFICATION OF REPORT | 18. SECURITY LASSIFICATION OF THIS PAGE | 19. SECURITY CLASSIFICATION OF ABSTRACT | 20. LIMITATION OF ABSTRACT |
|---|---|---|---|
| UNCLASSIFIED | UNCLASSIFIED | UNCLASSIFIED | UL |

MathSoft

# Wavelet-Based Analysis and Software for Multi-Scale Fractal Processes

## Air Force STTR

## Phase I Final Technical Report

Seattle Division of MathSoft, Inc.
1700 Westlake Ave. N, Suite 500
Seattle, WA 98109.9891, USA
Tel: (206) 283-8802
FAX: (206) 283-6310

E-mail: wconstan@statsci.com
dbp@statsci.com
jlu@statsci.com
reinhall@u.washington.edu
jbb@nsr.bioeng.washington.edu

# Contents

# 1 Technical Abstract

In this final technical report for the phase I Air Force STTR contract FQ8671-9901279, we summarize the technical objectives, work accomplished, results, and technical feasibility. The primary objective of this research is to develop methodology and software for the analysis of atmospheric turbulence and related data. Turbulence data are challenging because they are inherently non-stationary across a range of scales. Because the discrete wavelet transform is a natural tool for use with non-stationary and scale-dependent data, we investigated the efficacy of a variety of wavelet-based techniques including approximate maximum likelihood and least squares estimators. These estimators were adapted to work effectively in the presence of (i) slow variations in the power-law parameters, (ii) large scale stochastic trends and (iii) small scale non-turbulent events. The statistical properties of (most) wavelet-based power-law parameter estimators were examined and confidence intervals created. We assessed the efficacy of power-law models (which are proposed capture the salient features in actual turbulence measurements) by studying the variability in the wavelet coefficients at particular scales and comparing it to the variability that would occur if a time-varying power-law model were an adequate description. We also investigated the relevance of nonlinear deterministic modeling of wavelet sub-bands and used the technique for short-term prediction. All software was implemented in MathSoft's next generation S+WAVELETS module.

# 2 Introduction: Team Members and Phase I Publication Summary

## 2.1 Project Members

**Principal Investigator: William L. B. Constantine**, Research Scientist
Data Analysis Products Division of MathSoft, Inc., Seattle, WA

Dr. Constantine is in charge of all aspects of the project including software design, development and implementation. His expertise is in digital signal processing (with an emphasis in wavelets) and nonlinear dynamics.

**Investigator: Donald B. Percival**, Senior Mathematician
Data Analysis Products Division of MathSoft, Inc., Seattle, WA

Dr. Percival is an integral member of the phase I team and is an expert in wavelet theory, time series modeling, and spectral analysis techniques.

**Investigator: Z. Q. John Lu**, Research Scientist
Data Analysis Products Division of MathSoft, Inc., Seattle, WA

Dr. Lu is in charge of the development of (novel) deterministic modeling and prediction algorithms for the phase I contract. His principal area of expertise is in multivariate nonlinear regression, nonlinear time series analysis, and statistical modeling of fractal geometry.

**Consultant: Per G. Reinhall**, Professor
Department of Mechanical Engineering, University of Washington, Seattle

Dr. Reinhall is the lead investigator for the phase I academic partnership with the University of Washington. His area of expertise is in nonlinear dynamics and time series analysis, modeling of biological systems, vibrations and manufacturing.

**Consultant: James Bassingthwaighte**, Professor
Department of Bioengineering and Biomathematics, University of Washington, Seattle

Dr. Bassingthwaighte has played a supporting role in the development of new fractal time series algorithms and is considered an expert in biomedical fractal time series analysis.

**Academic Researcher: Peter Craigmile**, Ph.D. Candidate
Department of Statistics, University of Washington, Seattle

Peter has played a pivotal role in the development of stochastic modeling techniques for fractal (turbulence) time

series. His Ph.D. is focused on stochastic modeling of long memory processes.

## 2.2 Published Material

We made significant progress in our phase I research which has lead to the following publications:

• P. Craigmile, Percival, D.B. and Guttorp, P. (2000), "Wavelet-Based Parameter Estimation for Trend Contaminated Fractionally Differenced Processes," Technical Report for *National Research Center for Statistics and the Environment, University of Washington.*

• P. Craigmile, Percival, D.B. and Guttorp, P. (2000) *Decorrelation Properties of Wavelet Based Estimators for Fractionally Differenced Processes.* Proceedings of the $3^{rd}$ European Conference of Mathematics: Birkhäuser Verlag.

• P. Craigmile, Percival, D.B. and Guttorp, P. (2000), "Assessing Non-linear Trends using the Discrete Wavelet Transform," Technical Report for *National Research Center for Statistics and the Environment, University of Washington.*

• Peter F. Craigmile (2000) *Wavelet Based Estimation for Trend Contaminated Long Memory Processes.* Ph.D. Dissertation: University of Washington, Department of Statistics.

• W. Constantine, D.B. Percival, P.G. Reinhall, (2000). "Modeling Aerothermal Turbulence using Fractionally Differenced Processes," to be submitted to *Physical Review E* after approval from AFOSR Public Affairs.

• D. B. Percival and A. T. Walden (2000) *Wavelet Methods for Time Series Analysis.* Cambridge University Press.

These publications were fully or partially supported by this phase I contract.

# 3 Technical Objectives

The primary phase I research and development objectives are as follows.

1. *Review of models for non-stationary and multi-scale turbulence data.* Using actual turbulence measurements, we will evaluate the relative merits of three models for handling such data. The first is a stochastic model based directly on the octave-band decomposition given by the discrete wavelet transform (DWT), in which we seek to model each subband series in the decomposition using traditional time series methods (e.g., autoregressive models and generalizations thereof). The second is also a stochastic model and was used recently by Papanicolaou *et al.* [20]. This model treats turbulence as a time-evolving power law process whose exponent obeys a first order autoregressive model. The third model is based on the idea of representing turbulence as a deterministic multi-scale fractal process.

2. *Development of estimators for stochastic and deterministic fractal processes.* For the two stochastic models to be considered, we will investigate the relative merits of approximate maximum likelihood and least squares estimators of the relevant model parameters. We will investigate the effect on parameter estimation due to the wavelet that is chosen to form the DWT (the choice of wavelet is particularly important because, while it is tempting to use the Haar wavelet because of its inherent simplicity, we have found in working with other turbulence data [21] that the Haar wavelet does not work well for powers laws $f^{\alpha}$ with $\alpha \leq -2.5$ or for power laws observed in the presence of significant large scale stochastic or deterministic trends). For deterministic chaotic modeling of turbulence data, we will assess the applicability of nonlinear dynamic measures such as generalized fractal dimensions, Lyapunov exponents and approximate entropy.

3. *Development of analysis strategy.* We will develop an overall strategy for analyzing multi-scale fractal processes. This strategy will help guide the non-expert in their work and will influence the software design.

4. *Integration of methods into a user-friendly software environment.* We will implement the software needed for model evaluation and model estimation into MathSoft's next generation S+WAVELETS software.

# 4 Technical Approach and Accomplished Work

The last three decades have seen a rapid advance in the mathematical modeling of turbulence data. Encouraged partly by the fact that complex, seemingly random, behavior can be well modeled by simple low dimensional deterministic nonlinear systems, many researchers have hypothesized that turbulence can be modeled using chaos theory. Early experiments in Rayleigh-Bernard thermal convection [19], Taylor-Couette flow between cylinders [24], closed loop thermosiphons [3], turbulent boundary layers for open flow over a wall [1], and surface wave propagation in a saltwater medium [12], have in part verified this hypothesis. However, there is a lack of such clear proof in other experiments and in data collected from uncontrolled environments such as in aerothermal data. More recent efforts in turbulence modeling have shown chaos theory to be useful in interpreting local phenomenon and flow stability. Chaos is now generally considered to have an important (yet limited) role in the modeling of turbulence but not as a theory capable of describing turbulent flow in detail. Even if the turbulence is viewed as a deterministic event, the high degrees of freedom (dimension) of the flow makes the use of chaos theory impractical. Hence, the treatment of turbulence as a stochastic process prevails and (like low dimensional chaotic models) is well-matched for handling a prevalent notion about turbulence, namely, that it has certain 'self-similar' or 'fractal' properties. Loosely speaking, this property means that certain measures of turbulence data are invariant upon rescaling the data, but the measures are quite different for stochastic and deterministic models (e.g., invariance in distributional properties in the former and invariance in space-filling properties in the latter). Both approaches are capable of generating simulated series that mimic some properties of actual turbulence, but there is much work yet to be done to ascertain which class of models or combination thereof is the best to use to answer questions of practical importance.

Most deterministic and stochastic approaches assume homogeneity in time across all scales of interest. In this report, we discuss methods that can be used for turbulence with time-varying properties. As we show below, there is strong evidence to support the notion that turbulence exhibits time varying power law behavior over finite ranges of scale. Because of the temporally localized and scale dependent nature of wavelet transforms, wavelet techniques provide a natural framework for the analysis of physical phenomena that exhibit variations across time and within a finite range of scales. This is a departure from techniques that assume a priori either a self-similar structure across all scales in the data or stationarity in fractal measures as a function of time. While a wavelet decomposition of a turbulence time series, say $\{X_t\}$, is based on using self-similar analysis tools (i.e., wavelets), it does *not* make an a priori assumption that $\{X_t\}$ is evolving in a self-similar manner. By making a careful study of each scale as it evolves in time and of the relationships of the scales to each other, we can then evaluate how reasonable it is to use models that postulates a tight coupling across scales, e.g., a time-evolving power-law processes.

In our effort to address these issues, we use a stochastic fractal time series model known as a fractionally differenced process (FDP) [4]. An FDP has a clear advantage over similar models such as fractional Brownian motion (fBm) and fractional Gaussian noise (fGn) for the following reasons:

- UNLIMITED POWER LAW EXPONENT RANGE. Both fBm and fGn are stochastic power law processes in that their spectral density functions are approximately proportional to $|f|^{\alpha}$ where $\alpha$ is the power law exponent. However, an fBm is limited to an exponent range of $-3 < \alpha < -1$ while a fGn is limited to $-1 < \alpha < 1$. An FDP is also a stochastic power law process, but it has no such limitation on its exponent range and is theoretically valid for $\alpha \in \mathbb{R}$.

- MODEL CONTINUITY. Because fBm and fGn jointly cover power laws ranging from $-3$ up to 1 (which is adequate to model some – but not all – turbulent phenomena), it is tempting to select between fBm and fGn to model various turbulent series; however, at $\alpha = -1$ (which is known as $1/f$, pink, or flicker noise), there is a discontinuity between the fGn and fBm models at high frequencies, which can lead to problems in model selection. Unfortunately, many real world phenomena exhibit $1/f$ noise [2]. An FDP has no such discontinuity.

- TRACTABLE SDF AND ACVS. In contrast to the fBm and fGn models, an FDP has tractable forms for both its spectral density function (SDF) and (when stationary) corresponding autocovariance sequence (ACVS).

- MODEL FLEXIBILITY. Both autoregressive (AR) and moving average (MA) components can be added to an FDP to provide more flexibility in modeling high frequency spectral content. High end frequencies are typically contaminated by exogenous noise sources, and thus flexible modeling of these regions is appropriate. The fBm and fGn models are not *readily* amenable to such additions as it further complicates the SDF and ACVS functions.

In this report, we use recently developed wavelet techniques to estimate the parameters of FDP models applied to aerothermal turbulence data. There are a number of advantages in using the discrete wavelet transform (DWT) on turbulence data:

- DECOMPOSITION BASED ON SCALE. Turbulence is known to exhibit fluctuations at various spatial scales, and hence the DWT is a natural analyzer.
- DECORRELATION OF TIME SERIES. This is crucial for obtaining viable approximate maximum likelihood estimates of FDP parameters [6] (see Sec. 5.3.3 for details).
- LOCALIZED TIME AND SCALE CONTENT. Each wavelet coefficient is localized in time, allowing us to track changes in the characteristics of a time series at a particular scale as a function of time.
- SEPARATION OF NONLINEAR TRENDS FROM NOISE. The wavelet coefficients are inherently "blind" (invariant) to nonlinear polynomial trend contamination in the original time series [8, 7].

## 4.1 Theoretical Developments and Background

Here we develop the background and theory for the models and corresponding estimators used to analyze aerothermal turbulence data.

### 4.1.1 Fractionally Differenced Processes

An FDP is used to model data with a slowly decaying autocovariance function, a hallmark of long memory dependence. The process was originally proposed by Granger and Joyeux [10] and Hosking [11] as an extension to ARIMA$(0, \delta, 0)$ models to allow for fractional values of $\delta$.

**Definition 2.1** *Let $\delta \in \mathbb{R}$ and $\sigma_\varepsilon^2 > 0$. We say that $\{X_t\}_{t\in\mathbb{Z}}$ is an FDP$(\delta, \sigma_\varepsilon^2)$ if it has a spectral density function*

$$S_X(f) = \frac{\sigma_\varepsilon^2}{|2\sin(\pi f)|^{2\delta}}, \qquad |f| < 1/2, \tag{1}$$

*where $\sigma_\varepsilon^2$ is the innovation variance, and $\delta$ is the fractional difference parameter.*

When $-1/2 \leq \delta < 1/2$, an FDP is stationary with autocovariance sequence

$$s_{X,\tau} = \frac{\sigma_\varepsilon^2 \Gamma(1-2\delta)\Gamma(\tau+\delta)}{\pi\Gamma(\tau+1-\delta)}. \tag{2}$$

By inspection of Eq. 1, an FDP$(\delta, \sigma_\varepsilon^2)$ process approximately obeys a colored noise process ($S_X \propto |f|^\alpha$) at low frequencies with $\alpha = -2\delta$ (the error in this approximation is quite small for $|f| \leq 1/8$). This is an excellent model for data exhibiting power law behavior in both the stationary ($\delta < 1/2$) and nonstationary ($\delta \geq 1/2$) regimes. For $\delta \geq 1/2$ in Eq. 1, we obtain a class of nonstationary FDP that is stationary if $\{X_t\}$ is differenced $\lfloor \delta + 1/2 \rfloor$ times. More generally, an FDP is closed under differencing operations, i.e. an FDP$(\delta, \sigma_\varepsilon^2)$ that has been subjected to a $B^{th}$ order differencing operation, yields an FDP$(\delta - B, \sigma_\varepsilon^2)$. A pure power law process subjected to the same differencing operation will not yield another pure power law process, thus making an FDP a more flexible and robust model.

### 4.1.2 The Discrete Wavelet Transform

Consider a uniformly sampled time series $\{X_t\}_{t=0}^{N-1}$ with $N$ divisible by $2^J$ for $J \in \mathbb{N}$. For $L$ an even positive integer, let $\{h_l\}_{l=0}^{L-1}$ be a Daubechies [9] wavelet filter with squared gain function

$$\mathcal{H}_{1,L}(f) \equiv 2\sin^L(\pi f) \sum_{l=0}^{L/2-1} \binom{L/2-1+l}{l} \cos^{2l}(\pi f). \tag{3}$$

Equation 3 does not uniquely define a wavelet filter, and an additional phase criterion, such as *extremal* or *least asymmetric* phase, must be imposed to do so. Let $\{g_l\}_{l=0}^{L-1}$ be a *scaling* filter, defined by the quadrature mirror filter (QMF) relation

$$g_l = (-1)^{l+1} h_{L-1-l}. \tag{4}$$

The squared gain function for a Daubechies scaling filter is given by

$$\mathcal{G}_{1,L}(f) \equiv 2\cos^L(\pi f) \sum_{l=0}^{L/2-1} \binom{L/2-1+l}{l} \sin^{2l}(\pi f). \tag{5}$$

The wavelet and scaling filter are used in a "pyramid" algorithm [18] to transform $\{X_t\}$ into a collection of wavelet coefficients $W_{j,t}$ and scaling coefficients $V_{j,t}$ that can be grouped by physical scale $\tau_j \equiv 2^{j-1}\Delta t$ for $j = 1, \ldots, J$, where $\Delta t$ is the sampling time between contiguous observations in $\{X_t\}$ (for simplicity, we set $\Delta t$ to unity throughout this report for the mathematical derivation of FDP parameter estimators). The collection of coefficients $\mathbf{W}$, given by

$$\mathbf{W} = (\mathbf{W}_1, \mathbf{W}_2, \ldots, \mathbf{W}_J, \mathbf{V}_J) \tag{6}$$

where $\mathbf{W}_j$ are the $N_j \equiv N/2^j$ wavelet coefficients and $\mathbf{V}_J$ are the $N/2^J$ scaling coefficients, represents the discrete wavelet transform of $\{X_t\}$. Implementation of the DWT begins by defining the zeroth level scaling coefficients to be the original time series: $V_{0,t} \equiv \{X_t\}_{t=0}^{N-1}$. The level $j$ wavelet coefficients $W_{j,t}$ and scaling coefficients $V_{j,t}$ are then formed by

$$W_{j,t} \equiv \sum_{l=0}^{L-1} h_l V_{j-1,2t+1-l \bmod N_{j-1}} \text{ and } V_{j,t} \equiv \sum_{l=0}^{L-1} g_l V_{j-1,2t+1-l \bmod N_{j-1}} \tag{7}$$

where $t = 0, \ldots, N_j - 1$. The pyramid algorithm represented by Eq. 7 can also be interpreted as a series of cascade filter bank operations since the wavelet filter used to create the $W_{j,t}$ is an approximate bandpass filter with nominal pass-band $f \in [1/4\tau_j, 1/2\tau_j]$ while the corresponding scaling filter used to create the $V_{j,t}$ is a low pass filter with nominal pass-band $f \in [0, 1/4\tau_j]$. Figure 1 shows the squared gain responses for a 20-tap Daubechies wavelet filter $\mathcal{H}_{j,20}(f)$ and scaling filter $\mathcal{G}_{j,20}(f)$ for $j = 1, \ldots, 4$ and illustrates the filter bank perspective. When considering the statistical

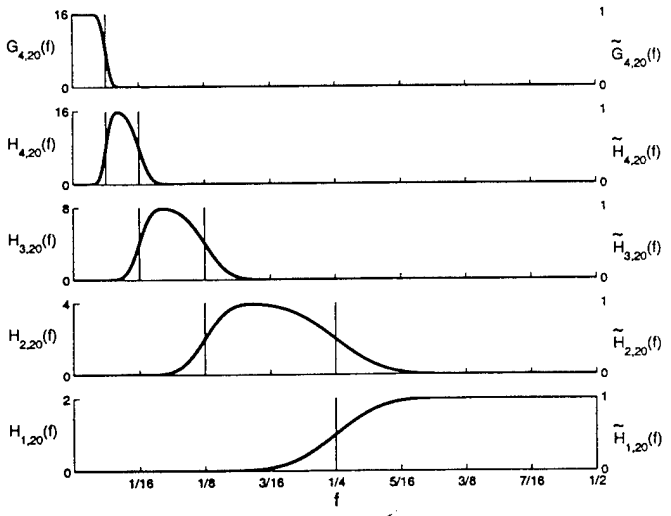


Figure 1: The squared gain functions for Daubechies least asymmetric 20-tap wavelet filter for levels $j = 1, \ldots, 4$. For simplicity, the sampling period was set to unity to create the frequency axis and establishes the Nyquist frequency at 1/2. The dotted vertical lines identify the octave bands over which the wavelet and scaling filters are associated. The scaling of the left (right) ordinate is representative of the DWT (MODWT) squared gain function.

properties of DWT coefficients, it is useful to divide the wavelet and scaling coefficients into *boundary* and *interior* coefficients. Boundary coefficients are those subject to change if the 'mod' operator were to be dropped in Eq. 7. These boundary coefficients must be ignored (for example) when calculating *unbiased* wavelet variance estimates (see Sec. 4.1.5 for details). The number of DWT boundary coefficients is given by $\min\{L_j, N_j\}$ where $L_j \equiv \lceil (L-2)(1-2^{-j}) \rceil$ (for large $j$, $L_j = L - 2$). The remaining DWT coefficients, of which there are $M_j \equiv N_j - \min\{L_j, N_j\}$, make up the set of interior coefficients. Figure 2 shows a DWT transform of a small segment of aerothermal data. A physical interpretation of the DWT based upon Daubechies' class of compactly supported wavelet filters is that the $W_{j,t}$ measure the *difference* (centered at a particular time) between adjacent weighted averages of $\{X_t\}$ at scale $\tau_j$. Large values for the $W_{j,t}$ indicate that $\{X_t\}$ tends to have large variations over time scales of length $\tau_j$. Similar to the wavelet coefficients, the scaling coefficients are weighted *averages* of $\{X_t\}$ on a scale of $\tau_j$.

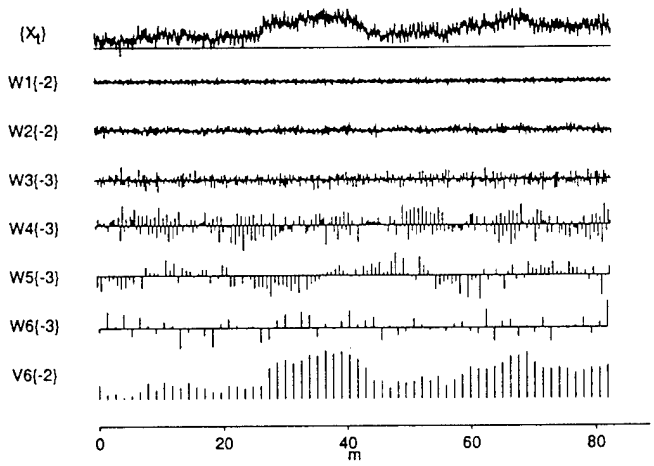


Figure 2: DWT of aerothermal data segment using Daubechies 8-tap least asymmetric filters. The number in the curly brackets next to each subband represents the amount of circular shift imposed to adjust the coefficients to approximate zero phase. A negative shift value implies an advance, or left circular shift, of the coefficients.

### 4.1.3 Maximum Overlap Discrete Wavelet Transform (MODWT)

Despite its popularity, the DWT has a few practical limitations:

- DYADIC LENGTH REQUIREMENT: The DWT can be adapted to accommodate arbitrary length sequences via polynomial extensions of the scaling coefficients. However, selecting an appropriate number of end points to fit or the order of fit is not a trivial task. Other, less complicated techniques may be used, but generally involve either a lot of bookkeeping or are too simple to accurately portray the dynamics of the scaling coefficients.
- LACK OF SHIFT INVARIANCE: The decimation operation makes the DWT a non shift-invariant transform.
- INAPPROPRIATE FOR INSTANTANEOUS TIME DEPENDENT MEASURES. The DWT coefficients represent too coarse of a "slicing" in the time domain to provide instantaneous FDP parameter estimates.

As an alternative, we can use a nondecimated form of the DWT, known as the maximum overlap DWT (MODWT) that has two main advantages: (1) it handles arbitrary length sequences inherently and (2) the MODWT coefficients can be circularly shifted to form an approximate zero phase projection of $\{X_t\}$ if the wavelet filter is approximate linear phase (as is the case for Daubechies least asymmetric and Coiflet filters). Additionally, the number of coefficients in each scale is equal to the number of points in the original time series. This refined slicing of the data in combination with the zero phase property allows us to calculate instantaneous statistical measures of the data across scale.

As in the DWT, implementation of the MODWT begins by defining the zeroth level scaling coefficients to be the original time series: $\widetilde{V}_{0,t} \equiv \{X_t\}_{t=0}^{N-1}$. Let $\widetilde{h}_l \equiv h_l/\sqrt{2}$ and $\widetilde{g} \equiv g_l/\sqrt{2}$ for $l = 0, \ldots, L-1$. The MODWT wavelet coefficients $\widetilde{W}_{j,t}$ and corresponding scaling coefficients $\widetilde{V}_{j,t}$ are formed by

$$\widetilde{W}_{j,t} \equiv \sum_{l=0}^{L-1} \widetilde{h}_l \widetilde{V}_{j-1,t-2^{j-1}l \bmod N} \quad \text{and} \quad \widetilde{V}_{j,t} \equiv \sum_{l=0}^{L-1} \widetilde{g}_l \widetilde{V}_{j-1,t-2^{j-1}l \bmod N} \tag{8}$$

where $j = 1, \ldots, J$ and $t = 0, \ldots, N-1$. The collection of coefficients $\widetilde{\mathbf{W}}$, given by

$$\widetilde{\mathbf{W}} = (\widetilde{\mathbf{W}}_1, \widetilde{\mathbf{W}}_2, \ldots, \widetilde{\mathbf{W}}_J, \widetilde{\mathbf{V}}_J) \tag{9}$$

where $\widetilde{\mathbf{W}}_j$ are the $N$ wavelet coefficients at scale $\tau_j$ and $\widetilde{\mathbf{V}}_J$ are the $N$ scaling coefficients at scale $\tau_J$, represents the MODWT of $\{X_t\}$. The number of boundary coefficients is $\widetilde{L}_j = (2^j - 1)(L-1) + 1$. Figure 3 shows a MODWT of aerothermal data using Daubechies 8-tap least asymmetric filters.

If the sample size $N$ is a power of two, the MODWT coefficients and DWT coefficients are related by

$$W_{j,t} = 2^{j/2}\widetilde{W}_{j,2^j(t+1)-1}. \tag{10}$$

The DWT can thus be seen as a scaled and subsampled version of the MODWT. This relation can be visualized, for example, by comparing the DWT scaling coefficients $V_{6,t}$ in Fig. 2 with the corresponding MODWT coefficients $\widetilde{V}_{6,t}$ in Fig. 3. Using Eq. 10, the MODWT squared gain functions are defined as $\widetilde{\mathcal{H}}(f) \equiv 2^{-j}\mathcal{H}(f)$ and $\widetilde{\mathcal{G}}(f) \equiv 2^{-j}\mathcal{G}(f)$ (see Fig. 1).

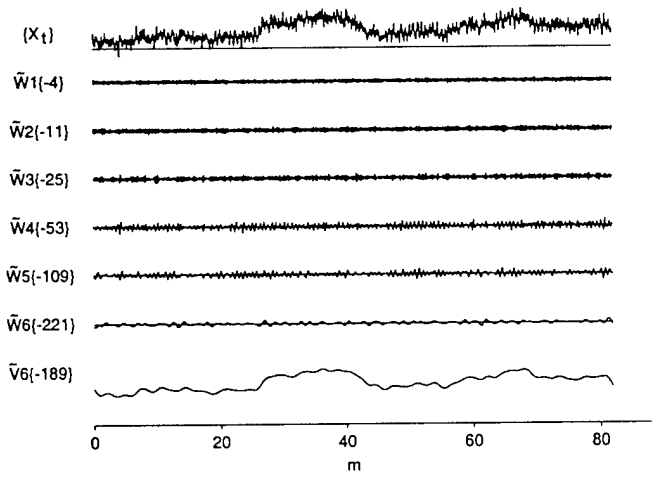


Figure 3: MODWT of aerothermal data segment using Daubechies 8-tap least asymmetric filters.

### 4.1.4 Time independent wavelet variance

### 4.1.5 MODWT wavelet variance

Since the SDF for the MODWT interior wavelet coefficients is given by $\widetilde{\mathcal{H}}_{j,L}(f)\ S_X(f)$, the variance of $\mathrm{var}\{\widetilde{W}_{j,t}\}$ can be expressed as

$$\mathrm{var}\{\widetilde{W}_{j,t}\} = \int_{-1/2}^{1/2} \widetilde{\mathcal{H}}_{j,L}(f) S_X(f)\ df. \tag{11}$$

Using the approximation that $\widetilde{\mathcal{H}}_{j,L}(f)$ is an ideal bandpass filter over $|f| \in [1/2^{j+1}, 1/2^j]$ and taking into consideration the even symmetry of SDFs, an approximation to the wavelet variance is given by

$$\mathrm{var}\{\widetilde{W}_{j,t}\} \approx 2\int_{1/2^{j+1}}^{1/2^j} S_X(f)\ df. \tag{12}$$

For fractional difference processes, we have

$$\mathrm{var}\{\widetilde{W}_{j,t}\} \approx 2\int_{1/2^{j+1}}^{1/2^j} \frac{\sigma_\epsilon^2}{|2\sin(\pi f)|^{2\delta}}\ df. \tag{13}$$

When $j \geq 3$, so that $\sin \pi f \approx \pi f$, Eq. 13 can be approximated by

$$\mathrm{var}\{\widetilde{W}_{j,t}\} \approx \sigma_\epsilon^2\ \widetilde{c}(\delta)\ \tau_j^{2\delta-1}, \tag{14}$$

where $\widetilde{c}(\delta) \equiv \pi^{-2\delta}(1 - 2^{2\delta-1})/(1 - 2\delta)$. Equation 14 suggests that a direct means of estimating $\delta$ is to fit a least squares line to the log of the estimated wavelet variance. The slope of the line, say $\beta$, that best fits $\log(\mathrm{var}\{\widetilde{W}_{j,t}\})$

versus $\log(\tau_j)$ in a least squares sense is related to the FDP parameter by $\delta = (\beta+1)/2$ and the pure power law (PPL) exponent by $\alpha = -(\beta+1)$.

For finite length time series, MODWT-based estimates of the wavelet variance are given by

$$\text{Biased: } \widetilde{\nu}_X^2 \equiv \frac{1}{N}\sum_{t=0}^{N-1} \widetilde{W}_{j,t}^2, \tag{15}$$

and

$$\text{Unbiased: } \widehat{\nu}_X^2 \equiv \frac{1}{\widetilde{M}_j}\sum_{t=\widetilde{L}_j-1}^{N-1} \widetilde{W}_{j,t}^2 \tag{16}$$

where $\widetilde{M}_j \equiv N - \widetilde{L}_j + 1$ is the number of MODWT interior wavelet coefficients. As a caveat, it should be noted that the wavelet variance estimates are somewhat sensitive to the order $L$ of the wavelet filter used in the analysis. In particular, studies by one of us [22] have shown that there can be a significant bias in the slope of the (2-tap) Haar wavelet variance estimates in log-log space due to a spectral leakage phenomenom. The leakage is attenuated as the filter order is increased, and the wavelet variance estimates typically stabilize for $L \geq 8$, as is true for all analyses presented in this report.

## 4.2 Development of fully-functional commercial-grade software

### 4.2.1 Enhancement of MathSoft's S+WAVELETS module

We have developed wavelet-based software written entirely in MathSoft's S-PLUS language to estimate parameters of a fractional difference (FD) process as a model for turbulence data. These functions will be incorporated directly into the S+WAVELETS module built for S-PLUS on UNIX platforms. The main functions developed thus far for the phase I contract are:

- WAVFDPMLE: Maximum likelihood (ML) estimation of FD parameters. This function optimizes a maximum likelihood functional to provide estimates of the FD parameter $\delta$ and innovation variance. The ML functional is approximated using discrete wavelet transform (DWT) coefficients and an internally defined FD spectral density function. This function has the ability to operate in detrending mode (nonlinear and nonstationary trends in the data are excluded) and recentering mode (the sample mean is removed from the data as a preprocessing measure). The user also has the option to choose a faster but slightly less accurate means of approximation (numerical integration of the spectral density function (SDF) is replaced by a band pass approximation scheme). Finally, the user is allowed to select the wavelet subbands over which the estimates are made.

- WAVFDPMLETIME: Time dependent ML estimation of the FD parameter $\delta$. This function calculates the local ML estimate of $\delta$ using MODWT coefficients. Biased and unbiased versions are available.

- WAVFDPWLSE: Weighted least squares estimate (WLSE) of the FD parameter $\delta$. This function calculates the weighted least squares power law exponent of MODWT wavelet variance estimates and converts it to $\delta$. The weights are calculated based on an assumption of a chi-square distribution. Biased and unbiased versions are available. The variance of the estimated $\delta$ is also returned.

- WAVFDPLSETIME: Time dependent least squares estimate of the FD parameter $\delta$. This function calculates the least squares instantaneous power law exponent of MODWT wavelet variance data and converts it to $\delta$. Biased and unbiased versions are available. The variance of the instantaneous $\delta$ estimates is also returned.

In addition to the above functions, the following helper functions were developed explicitly for (or greatly enhanced as a result of) the current phase I contract:

- WAVBOUNDARY: wavelet transform boundary coefficient separation.

- WAVCOVARIANCE: time (in)dependent (un)biased wavelet covariance estimation.

- WAVFDPBAND: mid-octave spectral density function evaluation using band-pass approximation.

- WAVFDPSDF: FDP spectral density function definition.

- WAVFDPTIMEINPUT: preprocessing function for time dependent FDP parameter estimation functions.
- WAVGAIN: general wavelet squared gain function development.
- WAVGAINDAUBECHIES: Daubechies wavelet squared gain response function.
- WAVHOMO: homogeneity of variance test.
- WAVINDEX: identification of wavelet boundary coefficients and zero-phase shift factors.
- WAVMODWT: maximum overlap discrete wavelet transform.
- WAVMODWTLONG: efficient MODWT for "large-scale" time series.
- WAVPERMUTE: permutation function for vector sequences.
- WAVSHIFT: wavelet zero phase shift function.
- WAVTITLE: extraction of series name for multiple classes.
- WAVVARIANCE: time (in)dependent (un)biased wavelet variance estimation.
- WAVVARIANCEINPUT: preprocessor for wavelet variance function.
- WAVZEROPHASE: calculation of zero phase shift indices for Daubechies' Coiflet and symmlet filters.

The functions are designed to take advantage of the object oriented nature of the S-PLUS language. Each of the functions listed above can accept input from a variety of classes including

- DWT: Discrete wavelet transform class.
- MODWT: Maximum overlap discrete wavelet transform class.
- MODWTLONG: Maximum overlap discrete wavelet transform class (long time series form).
- WAVEBOUND: Class containing wavelet transform coefficients separated into *boundary* and *interior* coefficients. The boundary coefficients are those subject to circular filtering operations and are excluded for unbiased and detrended FD parameter estimates. This class handles both DWT and MODWT class data
- WAVECOV: Wavelet covariance class.
- WAVEVAR: Wavelet variance class.
- TS: The S-PLUS language time series class.
- SIGNALSERIES: The S-PLUS language signal series class.
- NUMERIC: A vector of numeric data.

New classes are being developed for the functions described as well as plot, print, and summary methods which uniquely display the data in a way that is most relevant to the researcher.

# 5 Results

## 5.1 Aerothermal data collection

In this section we examine a uniformly sampled 7.5 million point aerothermal turbulence data set. Aerothermal data is a temperature (related) time series gathered by an aircraft flying at a constant elevation and constant speed. The measurement system is a cold-wire probe, externally attached to the aircraft, that senses fluctuations in local temperature by means of a proportional change in wire current. The data spans a total distance of 137.3 km with a spatial resolution of approximately 1.83 cm. For time dependent estimates of the FDP parameters, this large data set was divided into contiguous nonoverlapping $10,000$ point blocks and the series in each block analyzed. Figure 4 shows the aerothermal data smoothed with a moving average filter.

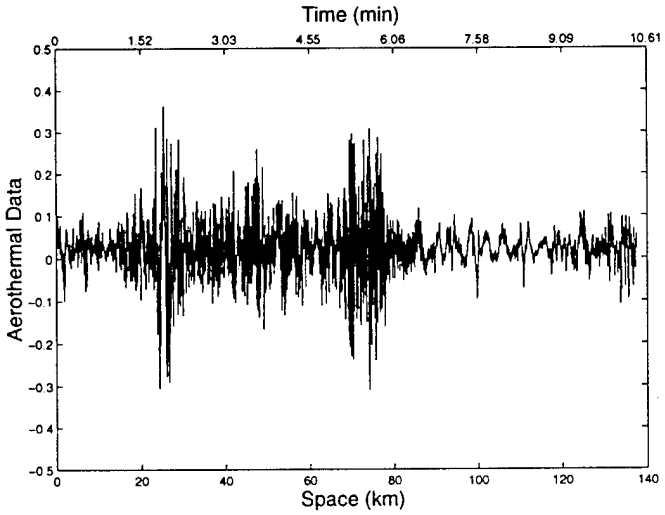


Figure 4: Moving average of the aerothermal data taken over 100 point nonoverlapping blocks.

## 5.2 Wavelet variance estimates

A time dependent wavelet variance estimator was used to assess the validity of power law scaling in turbulence data. Figure 5 shows an example of unbiased wavelet variance estimates for one 10,000 point block of aerothermal data. Multiscale linear trends in wavelet variance plots suggest the presence of spectral power law behavior. However, these trends appear only over finite ranges of scale. For the example shown in Figure 5, a different power law behavior is seen over scales $\tau_1 - \tau_4$, $\tau_5 - \tau_7$, and $\tau_8 - \tau_{10}$. These patterns change with different blocks, indicating time varying power law behavior.

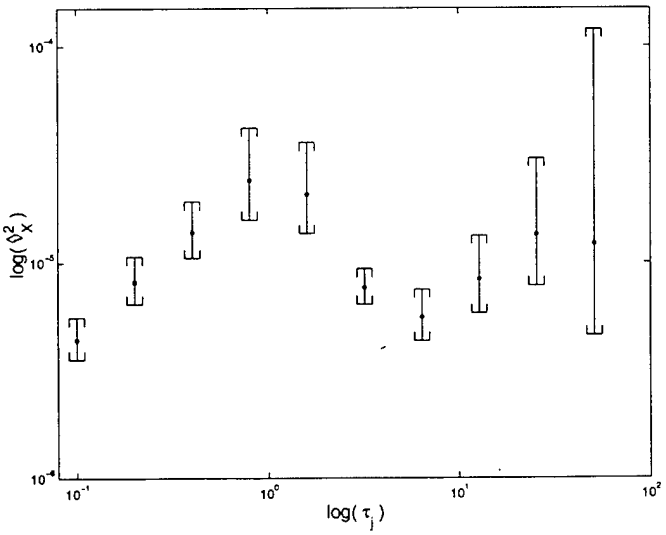


Figure 5: The unbiased MODWT wavelet variance $\hat{\nu}_X^2(\tau_j)$ of sample aerothermal data using Daubechies least asymmetric 8-tap wavelet filters. The confidence intervals are based on a chi-square distribution assumption where the equivalent degrees of freedom (EDOF) are calculated (1) using a large sample approximation to the mean and variance of $\hat{\nu}_X^2(\tau_j)$ for scales $\tau_1, \ldots, \tau_5$ and (2) under an assumption that the spectral density function is flat over the nominal passbands in which the wavelet coefficients are associated for $\tau_6, \ldots, \tau_{10}$. See [22] for details of wavelet variance confidence intervals and their development.

To better illustrate these pattern fluctuations, scatter plots of the wavelet variance estimates are shown in the lower

triangle of Fig. 6. We define $\mathbb{V}_{j,p} \equiv \log(\widehat{\nu}^2_{X,p}(\tau_j))$ for $j = 1, \ldots, 9$, with the index $p = 1, \ldots, P$ representing the $p^{th}$ 10,000 point nonoverlapping block in a uniform partition of the 7.5 million point aerothermal time series described in Sec. 5.1. A scatter plot $\Psi_{j,k}$ is produced by plotting $\mathbb{V}_{j,p}$ versus $\mathbb{V}_{k,p}$ for $j \neq k$. Inspection of Fig. 6 reveals a gradual spread in the wavelet variance estimates as we transverse scale from $\Psi_{1,2}$ to $\Psi_{8,9}$ off the main diagonal. This spread is proportional to the variation in $\delta$ over time. We can better characterize the spread in the scatter plots under the hypothesis that the var$\{\widetilde{W}_{j,t}\}$ obeys a FDP$(\delta, \sigma^2_\varepsilon)$. Taking the logarithm of Eq. 14, we obtain

$$\mathbb{V}_j \approx \log(\sigma^2_\varepsilon) + \log(\widetilde{c}(\delta)) + (j-1)(2\delta - 1), \tag{17}$$

that can be further simplified since $\log(\widetilde{c}(\delta))$ closely follows the tri-linear curve

$$\log(\widetilde{c}(\delta)) \approx \begin{cases} -1.60 - 2.90\ \delta & \text{if } \delta < -1, \\ -0.95 - 2.30\ \delta & \text{if } -1 \leq \delta \leq 2, \\ -2.10 - 1.70\ \delta & \text{if } \delta > 2. \end{cases} \tag{18}$$

As most physical power law processes are in the exponent range of $-4 < \alpha < 2$ (corresponding to $-1 < \delta < 2$), we can use a least squares linear approximation of $\log(\widetilde{c}(\delta))$ to reduce Eq. 17 to

$$\begin{aligned} \mathbb{V}_j &\approx [\log(\sigma^2_\varepsilon) + 0.05 - j] + 2(j - 2.15)\ \delta \\ &\equiv m_j + b_j \delta_j \end{aligned} \tag{19}$$

This approximation of $\mathbb{V}_j$ yields insight into the clustering of the data in the scatter plots. Any variation of the innovation variance or FDP parameter, for example, will cause estimates of $\mathbb{V}_j$ to migrate in the scatter plots. Hypothetically, if $m_j \approx m_k$ is constant and $b_j = b_k$ is allowed to vary over time, the points in the scatter plot will migrate at a slope $b_k/b_j = (k - 2.15)/(j - 2.15)$. This behavior can be seen for example in $\Psi_{6,7}$, $\Psi_{7,8}$ and $\Psi_{8,9}$ of Fig. 6. The lines in the lower triangle of Fig. 6 are drawn for reference with a slope of $b_k/b_j$ (under an FDP model, these lines are valid only for $j, k \geq 3$). If $b_j$ grows at a different linear rate than does $b_k$ for a fixed innovation variance, then the scatter plot will follow a curved path. These curved paths are particularly evident in $\Psi_{5,6}$ and $\Psi_{5,7}$. Finally, if neither $m_j$ nor $b_j$ vary much over time, the result is a small cluster of points in the scatter plot. This tightly coupled clustering can be seen, for example, in the upper triangle of Fig. 6 covering scales $\tau_1 - \tau_4$. An important implication of the scatter plots is to show that no single FDP can adequately model the turbulence data over all scales. Secondly, it is apparent that in many of the scatter plots for adjacent scales ($\Psi_{j,j\pm1}$) there is a convergence towards a linear trend at slope $b_j/b_{j\pm1}$, which is consistent with a power law coupling across those scales.

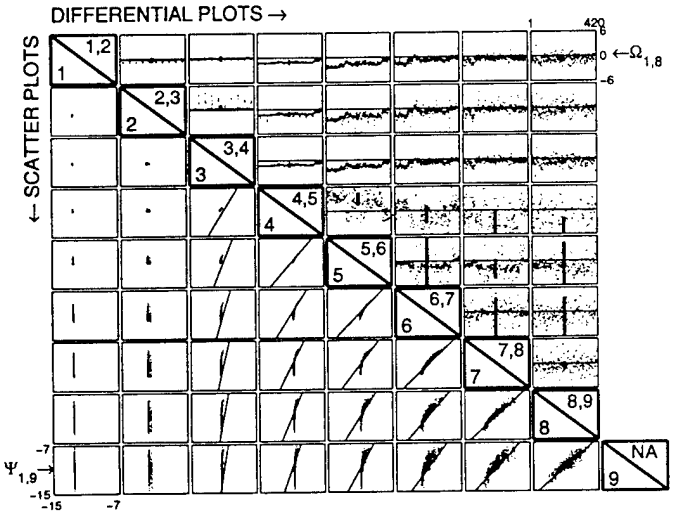


Figure 6: Scatter plots and differential scatter plots of $\log(\widehat{\nu}^2_{X,k}(\tau_j))$ estimates for $j = 1, \ldots, 9$ and $p = 1, \ldots, 420$. For purposes of comparison, all axes are uniformly scaled. See text for details.

We can also calculate "differential plots" $\Omega_{j,k}$ to gain insight on the coupling and variability of the estimated *slope* of the $\mathbb{V}_j$ relative to that of the $\mathbb{V}_k$. Define $\mathbb{D}_{j,p} \equiv \mathbb{V}_{j+1,p} - \mathbb{V}_{j,p}$ to be a gross approximation of the (log) wavelet

variance slope between scales $\tau_j$ and $\tau_{j+1}$ for $j = 1, \ldots, J-1$ in the $p^{th}$ data block for $p = 1, \ldots, P$. The differential scatter plot $\Omega_{j,k}$ is produced by plotting the statistic $d_{j,k,p} \equiv \mathbb{D}_{j,p}/\mathbb{D}_{k,p} - 1$ versus the block number $p$. The $\Omega_{j,k}$ qualitatively track the coupling of the slopes $\mathbb{D}_j$ and $\mathbb{D}_k$ as the block number (time) varies and are plotted in the upper triangle of Fig. 6. If $d_{j,k,p} = 0$, then the slopes are tightly coupled and suggests that a power law model is appropriate over the corresponding scales. An example of this behavior is seen in plots $\Omega_{1,2}$, $\Omega_{1,3}$ and $\Omega_{2,3}$ as they all fall close to the reference zero line. If $d_{j,k,p} \neq 0$ consistently over all blocks, then the two slopes are not consistent with a power law relationship. This behavior is seen, for example, in plots $\Omega_{j,4}$ and $\Omega_{j,5}$ for $j = 1, \ldots, 3$. To quantify the distribution of the data in the $\Omega_{j,k}$, each plot is overlaid with a boxplot whose thick-lined center represents the mean while the top and bottom of the box spans an estimate of 2 sample standard deviations about the mean.

Using the results shown in Fig. 5 and 6, we propose to fit separate FDP models to the aerothermal turbulence data over 4 finite ranges of scales: $\tau_1 - \tau_3$, $\tau_2 - \tau_4$, $\tau_5 - \tau_7$, and $\tau_8 - \tau_{10}$. The overlap of the first two scale ranges is purposely set to explore the apparent periodicities appearing in scales $\tau_3$ and $\tau_4$ (see $\Omega_{2,3}$ for example in Fig. 6). In what follows, we discuss wavelet-based time independent and dependent estimates for the FDP parameters via least squares and maximum likelihood techniques.

## 5.3 Estimating FDP parameters with wavelets

### 5.3.1 Block dependent weighted least squares estimator

Here we develop a weighted least squares estimator for $\delta$ based upon the unbiased MODWT-based wavelet variance estimator $\hat{\nu}_X^2(\tau_j)$ at scales $\tau_j$. The distribution for $\hat{\nu}_X^2(\tau_j)$ is approximately that of a chi-squared random variable $\chi_{\eta_j}^2 \hat{\nu}_X^2(\tau_j)/\eta_j$, where $\eta_j$ is the equivalent degree of freedom (Sec. 8.4 of [22] discusses three methods for determining $\eta_j$, the simplest of which is to set $\eta_j = \max\{\widetilde{M}_j/2^j, 1\}$). Define

$$Y(\tau_j) \equiv \log(\hat{\nu}_X^2(\tau_j)) - \psi\left(\frac{\eta_j}{2}\right) + \log\left(\frac{\eta_j}{2}\right) \tag{20}$$

where $\psi(\cdot)$ is the digamma function. We can now formulate a linear regression model $Y(\tau_j) = \gamma + \beta \log(\tau_j) + e_j$ where $e_j \equiv \log(\hat{\nu}_X^2(\tau_j)/\nu_X^2(\tau_j)) - \psi(\eta_j/2) + \log(\eta_j/2)$ is an error term with zero mean and variance $\psi'(\eta_j/2)$ ($\psi'(\cdot)$ is the trigamma function) [22]. The weighted least squares estimate (WLSE) of the slope term $\beta$ is

$$\hat{\beta}_{wlse} = \frac{\sum \omega_j \sum \omega_j \log(\tau_j) Y(\tau_j) - \sum \omega_j \log(\tau_j) \sum \omega_j Y(\tau_j)}{\sum \omega_j \sum \omega_j \log^2(\tau_j) - (\sum \omega_j \log(\tau_j))^2} \tag{21}$$

where $\omega_j \equiv [\psi'(\frac{\eta_j}{2})]^{-1}$. All sums in Eq. 21 are over $j = J_0, \ldots, J_1$. The weighted least squares estimate of the FDP parameter is then

$$\hat{\delta}_{wlse} = \frac{1}{2}(\hat{\beta}_{wlse} + 1). \tag{22}$$

Furthermore, the variance of $\hat{\beta}_{wlse}$ is

$$var\{\hat{\beta}_{wlse}\} = \frac{\sum \omega_j}{\sum \omega_j \sum \omega_j \log^2(\tau_j) - (\sum \omega_j \log(\tau_j))^2} \tag{23}$$

and thus the variance of the $\delta_{wlse}$ estimate is found by

$$var\{\hat{\delta}_{wlse}\} = \frac{1}{4} var\{\hat{\beta}_{wlse}\}. \tag{24}$$

Figures 7 and 8 show the weighted least squares estimates of $\alpha$ for the segmented turbulence data set described in Sec. 5.1. The power law exponent was estimated over finite ranges of scale, commensurate with those deemed appropriate by inspection of the wavelet variance estimates (Fig. 5 for example) and corresponding scatter plots (Fig. 6). Due to the sampling variability present in the wavelet variance estimates, we smoothed all $\hat{\alpha}_{wlse}$ for scales $\tau_j$ such that $j \geq 5$ with a moving average 20 point window with a 19 point overlap. For reference and simplicity, we define the term $\hat{\alpha}_{j,k}$ to mean the estimated power law exponent over scales $\tau_j, \tau_{j+1}, \ldots, \tau_k$. Figure 7 shows the estimates $\hat{\alpha}_{1,3}$, $\hat{\alpha}_{2,4}$ and $\hat{\alpha}_{5,7}$. An immediate observation of these results is the apparent wide range of $\alpha$ for various scales, spanning stationary blue noise to nonstationary red noise. This clearly suggests that a single (Kolmogorov) exponent is not an adequate description of this aerothermal turbulence data. Also apparent is a strong coupling between $\hat{\alpha}_{1,3}$

and $\hat{\alpha}_{2,4}$, which share a similar baseline value falling between the theoretical Kolmogorov exponent ($\alpha = -5/3$) and a random walk ($\alpha = -2$), but differ greatly in the periodicities found in $\hat{\alpha}_{2,4}$ (see also the $\Omega_{2,3}$ plot of Fig. 6). These periodicities are suspected to be due to an exogenous factor unrelated to aerothermal turbulence such as a periodic autopilot correction, inducing a local vibration (and corresponding recorded temperature fluctuation) in the cold wire probe instrumentation. For a relatively small segment of data near 5.5 minutes, there is a close convergence of the $\hat{\alpha}_{wlse}$ indicating the presence of a PPL persistent over many scales. Figure 8 shows the long scale estimates $\hat{\alpha}_{8,10}$ along with $\hat{\alpha}_{5,7}$ for purposes of comparison. Here we see that the long scale trends are only moderately coupled, suggesting once again that different power laws govern different ranges of scale and that the power law exponent is time dependent.

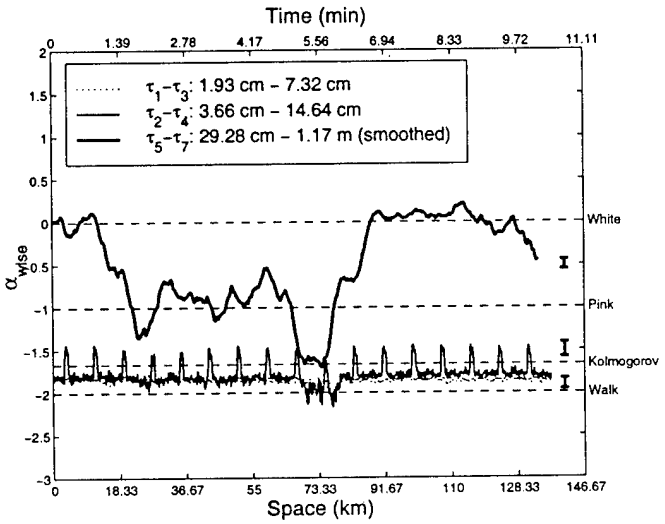


Figure 7: Weighted least squares estimates of the pure power law exponent $\alpha$ over scales $\tau_1 - \tau_7$ for the turbulence data.

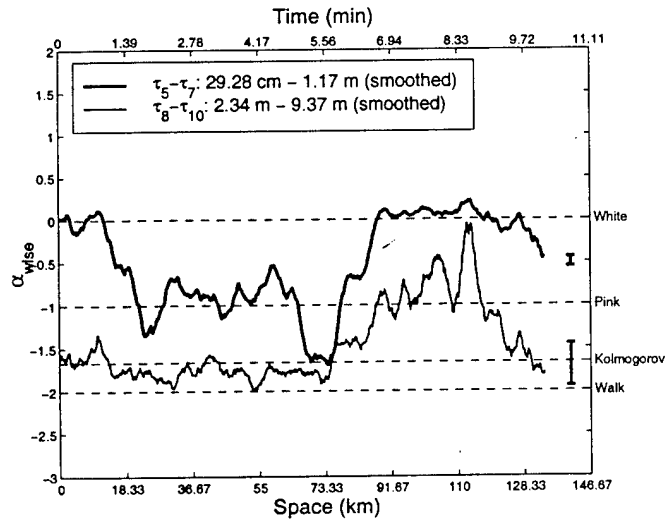


Figure 8: Weighted least squares estimates of $\alpha$ over scales $\tau_5 - \tau_{10}$ for the turbulence data.

### 5.3.2 Block independent least squares estimator

To form instantaneous least squares estimates of $\delta$ we use only a single wavelet coefficient from each scale, i.e., we use $\widetilde{W}_{j,t_j}$ where $t_j$ is the time index of the $j^{th}$ level MODWT coefficient associated with time $t$ in $\{X_t\}_{t=0}^{N-1}$. The time index $t_j$ can be meaningfully determined *only* if (approximate) linear phase wavelet filters are used. Using only the $\widetilde{W}_{j,t_j}$, the time dependent form of Eq. 22 becomes

$$\hat{\delta}_{wlse,t} = \frac{1}{2}\left(\frac{(J_1 - J_0 + 1)\sum \log(\tau_j) Y_t(\tau_j) - \sum \log(\tau_j) \sum Y_t(\tau_j)}{(J_1 - J_0 + 1)\sum \log^2(\tau_j) - (\sum \log(\tau_j))^2} + 1\right) \tag{25}$$

where all sums are over $j = J_0, \ldots, J_1$ and

$$Y_t(\tau_j) \equiv \log(\widetilde{W}_{j,t_j}^2) - \psi(1/2) - \log(2). \tag{26}$$

To decrease the variability of the estimates, the level $J_1$ is set to be as high as possible.

Figure 9 shows the $\hat{\alpha}_{wlse,t}$ (smoothed with a moving average filter) for the entire turbulence time series over scales $\tau_5 - \tau_7$. The smoothed $\hat{\alpha}_{wlse,t}$ follow the same patterns exhibited by $\hat{\alpha}_{5,7}$ shown in Fig. 8 and 11 with a bit more variability in the estimates. These variabilities are not captured by the block dependent estimators and illustrates the importance of using time dependent estimators for a more accurate portrayal of the (turbulence) dynamics.

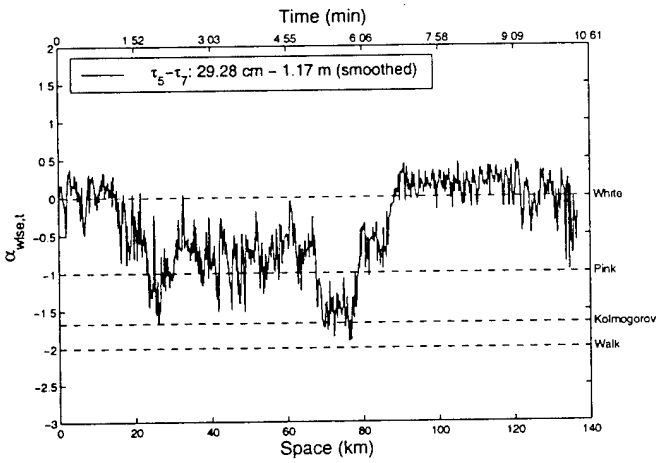


Figure 9: Unbiased $\hat{\delta}_{wlse,t}$ for the entire 7.5 million point turbulence record. A moving average filter was used to smooth the results using nonoverlapping 10,000 point windows.

### 5.3.3 Block dependent maximum likelihood estimator

Wavelet-based maximum likelihood techniques can be used in harmony with an FDP model as another means of obtaining estimates for FDP parameters. Suppose $\mathbf{X} = \{X_t\}_{t=0}^{N-1}$ can be regarded as a portion of a zero mean stationary FDP with unknown parameters $\delta$ and $\sigma_\epsilon^2 > 0$. Assuming that $\mathbf{X}$ obeys a multivariate Gaussian distribution, we can estimate $\delta$ and $\sigma_\epsilon^2$ by maximizing the likelihood function

$$\mathcal{L}(\delta, \sigma_\epsilon^2 | \mathbf{X}) \equiv \frac{1}{(2\pi)^{N/2} |\Sigma_\mathbf{X}|^{1/2}} e^{-\mathbf{X}^T \Sigma_\mathbf{X}^{-1} \mathbf{X}/2}, \tag{27}$$

where $\Sigma_\mathbf{X}$ is the covariance matrix of $\mathbf{X}$, and $|\Sigma_\mathbf{X}|$ is the determinant of $\Sigma_\mathbf{X}$. Note that the dependence of the likelihood function on $\delta$ and $\sigma_\epsilon^2$ is through $\Sigma_\mathbf{X}$ alone. In a practical setting however, evaluation of $\mathcal{L}(\delta, \sigma_\epsilon^2 | \mathbf{X})$ is computationally expensive even for moderate $N$ [4]. Secondly, numerical instabilities can occur when calculating the likelihood function close to $\delta = 1/2$.

An approximation to the likelihood function can be calculated using DWT coefficients. Using the DWT is advantageous in that it is known to decorrelate (long memory) FDP and related processes, forming a near independent

Gaussian sequence, and simplifying the statistics significantly [6]. The decorrelation property allows us to form a *reduced log likelihood* function without much computational burden:

$$\hat{l}(\delta, \tilde{\sigma}_\varepsilon^2(\delta)|\mathbf{X}) - N = N \log(\tilde{\sigma}_\varepsilon^2(\delta)) + \log(C'_{J+1}(\delta)) + \sum_{j=1}^{J} N_j \ \log(C'_j(\delta)) \tag{28}$$

where

$$\tilde{\sigma}_\varepsilon^2(\delta) \equiv \frac{1}{N}\left(\frac{V_{J,0}^2}{C'_{J+1}(\delta)} + \sum_{j=1}^{J} \frac{1}{C'_j(\delta)} \sum_{t=0}^{N_j-1} W_{j,t}^2\right) \tag{29}$$

and $C'_j(\delta)$ is the average SDF value at the mid-frequency of the band corresponding to DWT scale $\tau_j$ (see [22] for explicit details on the development of the reduced log likelihood function using the DWT coefficients). For our purposes, the mid-octave values are calculated using the SDF defined by Eq. 1. Minimizing Eq. 28, which is strictly a function of $\delta$, yields the maximum likelihood estimates of $\hat{\sigma}_{\varepsilon_{mle}}^2$ and $\hat{\delta}_{mle}$.

The variance of $\hat{\delta}_{mle}$ can be calculated as follows: let $\mathbf{W_I}$ be an $M = \sum_j M_j$ point vector containing all of the interior DWT wavelet coefficients. Assuming that the coefficients in $\mathbf{W_I}$ are uncorrelated and that $\delta \in [-1/2, L/2]$, then for large $N$ the estimator $\hat{\delta}_{mle}$ is approximately Gaussian distributed with mean $\delta$ and variance

$$\sigma_{\hat{\delta}_{mle}}^2 \equiv 2\left[\sum_{j=1}^{J} M_j \phi_j^2 - \frac{1}{M}\left(\sum_{j=1}^{J} M_j \phi_j\right)^2\right]^{-1} \tag{30}$$

where

$$\phi_j = -\frac{4\sigma_\varepsilon^2}{\text{var}\{W_{j,t}\}} \int_0^{1/2} \mathcal{H}_{j,L}(f) \frac{\log(2\sin(\pi f))}{[2\sin(\pi f)]^{2\delta}} \ df. \tag{31}$$

The term $\text{var}\{W_{j,t}\}$ is the process wavelet variance defined as

$$\text{var}\{W_{j,t}\} \equiv 2\int_0^{1/2} \mathcal{H}_{j,L}(f) S_X(f) \ df = 2\int_0^{1/2} \mathcal{H}_{j,L}(f) \frac{\sigma_\varepsilon^2}{[2\sin(\pi f)]^{2\delta}} \ df. \tag{32}$$

In practice, the integrals in Eq. 31 and 32 can be approximated through numerical integration or, based on the view that the wavelet transform forms an octave band decomposition (see Fig. 1), through a Taylor series expansion about the mid-octave frequencies for levels $j = 1, 2$ and direct integration using a small angle assumption for $j > 2$. There is generally a large increase in computational speed when using the bandpass approach with a relatively small loss of accuracy.

Figures 10 and 11 show the maximum likelihood estimates of $\alpha$ for the segmented turbulence data set described in Sec. 5.1. The $\hat{\alpha}_{mle}$ compare quite well with the $\hat{\alpha}_{wlse}$ (see Fig. 7 and 8) with the exception of the $\hat{\alpha}_{1,3}$ and $\hat{\alpha}_{8,10}$ estimates. The difference in $\hat{\alpha}_{1,3}$ is directly attributed to the difference in models. The weighted least squares estimates are based upon a pure power law model while the maximum likelihood estimates are based on an FDP whose SDF adheres to a power law for $f \leq 1/8$, but diverges from this behavior for $1/8 < f < 1/2$, corresponding to wavelet scale $\tau_1$ and, to a lesser extent, $\tau_2$. Figure 12 demonstrates the departure of an FDP SDF from that of a pure power law process. The difference in $\hat{\alpha}_{8,10}$ estimates is mainly due to a high degree of sampling variability in the wavelet variance estimates at long scales. In particular, at scale $\tau_{10}$ the number of DWT wavelet coefficients is diminished to $N_{10} = 10^4/2^{10} \approx 10$, i.e. a very small set of coefficients to obtain the $\hat{\alpha}_{mle}$.

### 5.3.4 Block independent maximum likelihood estimator

The MODWT coefficients can be circularly permuted to form an approximate zero phase decomposition using Daubechies' least asymmetric or Coiflet filters. Using the permuted coefficients $\widetilde{W}_{j,t_j}$, a reduced log-likelihood function can be minimized to form an "instantaneous" MLE of the FDP parameter $\delta$. The reduced likelihood function consists of a collection of wavelet coefficients, one from each scale, that are colocated in time and is defined as

$$\hat{l}_t(\delta|X) \equiv J \log\left(\frac{1}{J}\sum_{j=1}^{J} \frac{2^j}{C'_j(\delta)} \widetilde{W}_{j,t_j}\right) + \sum_{j=1}^{J} \log(C'_j(\delta)). \tag{33}$$

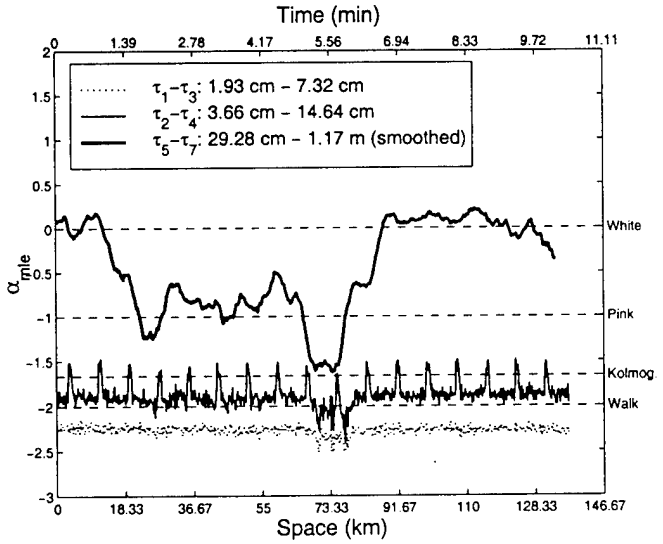


Figure 10: Maximum likelihood estimates of the pure power law exponent $\alpha$ over scales $\tau_1 - \tau_7$ for the turbulence data.

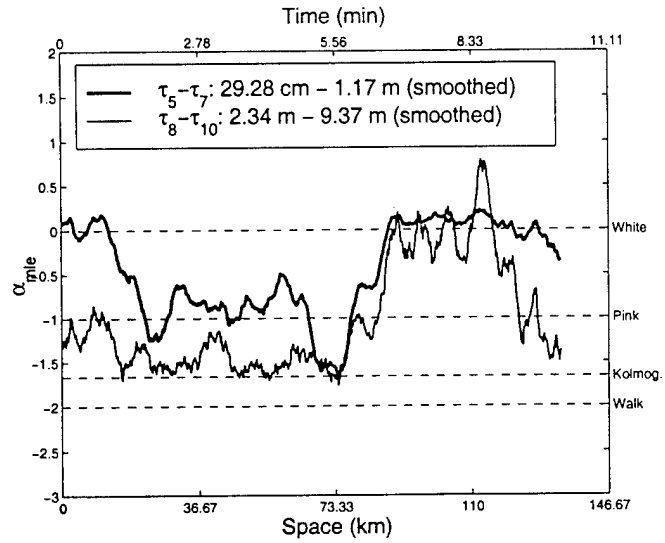


Figure 11: Maximum likelihood estimates of $\alpha$ over scales $\tau_5 - \tau_{10}$ for the turbulence data.

This approach is useful for processes that exhibit a variation in power law behavior over time. Figure 13 shows an example of unbiased $\hat{\delta}_{mle,t}$ for a small segment of aerothermal turbulence data. The results indicate a modest fluctuation of $\hat{\delta}_{mle,t}$ about a mean value of $\bar{\hat{\delta}}_{mle,t} = 1.04$ corresponding to a near-red noise $\bar{\hat{\alpha}}_{mle,t} = -2.08$. The estimated density function (Fig. 13(b)) and quantile-quantile (Q-Q) plot with respect to a normal density (Fig. 13(d)) both indicate a near Gaussian distribution of the $\hat{\delta}_{mle,t}$ estimates. The "S" shape in the Q-Q plot implies that the density function of the $\hat{\delta}_{mle,t}$ has longer tails than does a Gaussian.

### 5.3.5 Discussion of FDP parameter estimations

In this report we have introduced four wavelet based techniques to estimate FDP model parameters for aerothermal turbulence data: time (in)dependent weighted least squares estimators and time (in)dependent maximum likelihood estimators. For the time independent techniques, results were calculated for a 7.5 million point aerothermal data set taken in contiguous nonoverlapping 10,000 point intervals. The time independent results verify the presence of time

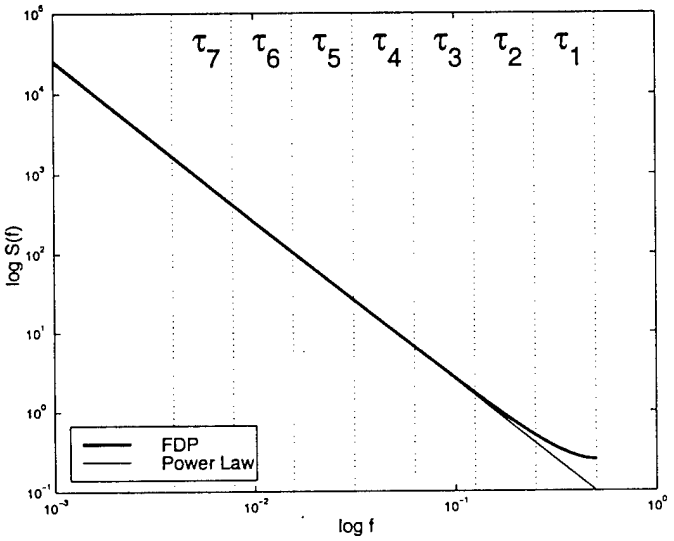


Figure 12: Spectral density functions for an FDP realization with $\delta = 1$ and a pure power law process with $\alpha = -2$. The vertical lines represent the division in octaves corresponding to various wavelet scales.

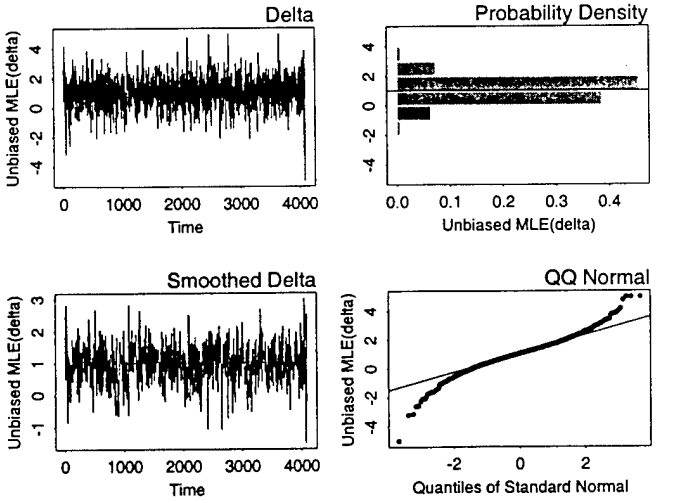


Figure 13: Unbiased $\hat{\delta}_{mle,t}$ for a sample segment of aerothermal data. Only the scales $\tau_1 - \tau_4$ were used for this estimation. Shown in the figure are (a) $\hat{\delta}_{mle,t}$ with 95% confidence intervals, (b) the corresponding estimated probability density, (c) a smoothed (low pass filtered) version of $\hat{\delta}_{mle,t}$ with confidence intervals and (d) a Q-Q plot of the $\hat{\delta}_{mle,t}$ with respect to a normal distribution.

varying power law processes with a power law exponent spanning stationary blue noise to nonstationary red noise and applicable over *finite* and *distinct* ranges of scale. The time dependent results were calculated for a small (4096 point) aerothermal data segment. These "instantaneous" estimators are very useful for detection of changes in system whose dynamics fluctuate rapidly as a function of time or scale. For time independent estimates, we introduce methods for calculating the variance of FDP parameters, that, under a chi-squared distribution assumption made on the variance of the wavelet coefficients, can be related to confidence intervals.

We showed in our research that in order to provide consistent results between maximum likelihood and weighted least squares estimates of the FDP parameter $\delta$, one needs to be aware of the divergence of the FDP spectral density function from that of a pure power law process at high frequencies (small scales). As a course of future research we intend to augment an FDP with an ARMA model for small scale variations, providing more flexibility than either a

pure power law or FDP model alone.

The collection of results supports the efficacy and validity of using stochastic FDP models for aerothermal turbulence data. The use of wavelet techniques allows us to examine the apparent self-similar behavior of turbulence over distinct and finite ranges of scale, and, when used with approximate linear phase wavelet filters, provides an effective means of characterizing time varying power law processes.

## 5.4 Wavelet-based forecasting for non-stationary multi-scale fractal processes

### 5.4.1 Nonlinear deterministic modeling of wavelet subband processes

To complement stochastic subband modeling, we assessed the efficacy of *deterministic nonlinear* modeling for aerothermal turbulence data. Figure 14 suggests one possible path to take for modeling and prediction of subband processes via wavelet techniques. The original time series is fed into (a form of) the discrete wavelet transform to produce the subband processes $W_{j,t}$. A portion of the $W_{j,t}$ coefficients are used for training the prediction algorithm based on stochastic and deterministic models to produce a predicted set of coefficient. These predicted coefficients are then augmented with the training set and an inverse wavelet transform performed to yield a predicted time series. The hypothesis is that the inverted series will have better predictive power than those techniques based on the original series alone. This flexible scheme is relevant to analysis of turbulence data in three important ways:

1. Wavelet transforms can be used to decompose a complex, possibly nonstationary and multi-scale series into a few crystals (a 'crystal' is a set of wavelet coefficients at a particular scale), each of which has its own dynamical and statistical behavior, and different prediction techniques can be applied separately to each crystal.

2. The implicit differencing operations of wavelet filters can be used to analyze nonstationary sequences with stationary backward differences. The stationarity of the wavelet coefficients provides a means of generating useful statistics on the data.

3. Using approximate linear phase wavelet and scaling filters, the nondecimated versions of the wavelet transform (MODWT, MODWPT) can be used to meaningfully colocate the wavelet coefficients with events in the original series (an important feature for the modeling of cross-scale components).

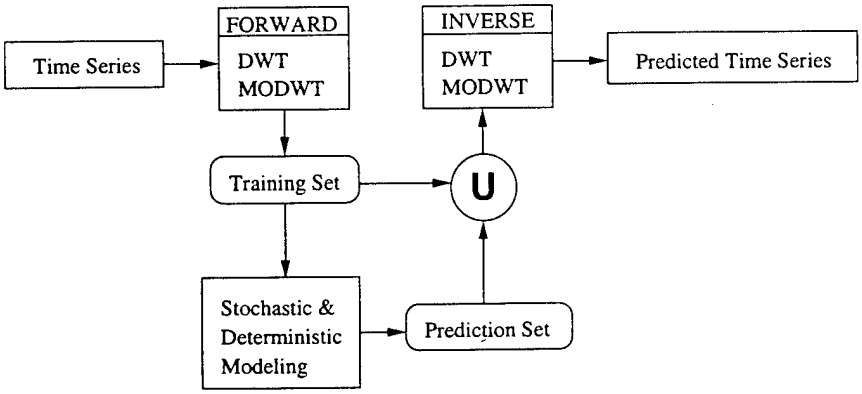


Figure 14: Flow chart for subband modeling and prediction.

or phase I, we implemented the scheme outlined in Fig. 14 using nonlinear dynamic models on preselected subbands of a MODWT decomposition. In nonlinear dynamics, a quick means of detecting deterministic structure in a time series is through lag plots, produced by plotting a time series versus a shifted version of itself. We refer to the data in these plots as being *embedded*. A "fuzzy" or cloudy clustering of points in the embedding suggests the presence of either a high dimensional deterministic structure or a stochastic structure in the data. Conversely, well defined patterns in the embeddings suggest an underlying deterministic structure. Figure 15 shows sample lag plots for three wavelet crystals. Deterministic structure can be seen in the embeddings of the $d_5$ and $d_7$ crystals while a stochastic clutter is seen in the embedding for $d_1$; illustrating the need for a combination of stochastic and deterministic modeling in the subbands.

As a preliminary investigation, we applied the prediction technique outlined in Fig. 14 to a 3000 point *sunspots* series which is known to have strong deterministic components mixed with colored noise. We isolated the deterministic cyclical components from the noise via a MODWT of the data. We then hypothesized that the cyclical variations were

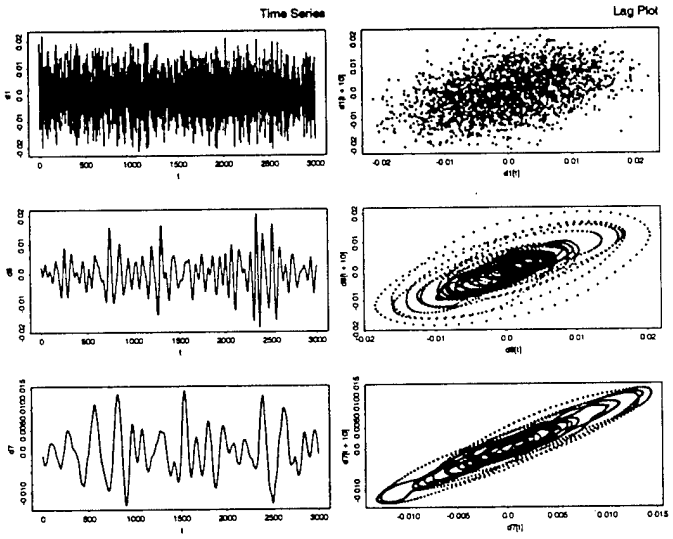


Figure 15: Time histories and phase plane embeddings of MODWT wavelet crystals $d1$, $d5$, and $d7$. The data is a 3000 point subset of the aerothermal turbulence data.

well modeled by a nonlinear deterministic system and used a relevant nonlinear technique, the local Lyapunov exponent (LLE) prediction method developed by one of us [14, 15, 13], to predict the latter third of the of the data using the first two thirds as a training set. The LLE technique was applied to crystals which displayed deterministic patterns in the phase plane. For prediction within each "stochastic crystal", the sample mean of training set was extended as an ersatz prediction of future values. This allowed us to independently test the prediction capabilities of the LLE in the context of wavelet subband processing. The predicted wavelet coefficients were augmented with the training coefficients, and the inverse MODWT applied. We refer to the predicted time series as a *local Lyapunov wavelet synthesis (LLWS)*. For purposes of comparison, a commonly known nonlinear technique known as *nearest neighbor (NN)* prediction, was applied to the original time series. Preliminary results indicate that the LLWS approach achieves better prediction accuracy than the traditional NN algorithm as the magnitudes and phases of the sunspots series are better fit by the LLWS. The NN prediction of the original series (only) fails to predict the high amplitude sunspot variations (Fig. 16). The smoothness of the LLWS of sunspots data is simply due to the fact that a constant was used for the predicted coefficients in noisy subbands. An obvious improvement to the technique would be to apply a reasonable stochastic model to the noisy wavelet crystals. In phase II, we plan to refine the technique by testing an ensemble of stochastic and deterministic subband models during the remainder of the phase I contract.

Based on the results shown in Fig. 15 and 16, we suggest that it is feasible to use nonlinear deterministic prediction in the context of wavelet subband modeling. The efficacy of the prediction is a direct function of the level of noise in the data. We therefore suggest that this technique would be most effective for large-scale variations present in turbulence time series.

# 6 Estimates of Technical Feasibility

In order to address the technical feasibility of our work in phase I, we summarize the relationship with future research and development, discuss the commercial potential of the product into the current S+WAVELETS module and a (possible) Matlab toolbox. We close with a company mission and product line and summarize our commercialization record.

## 6.1 Relationship with Future Research and Development

Our phase I research has resulted in new 'blocked' and 'local' schemes for estimating the parameters of a non-stationary multi-scale fractal process and for attaching confidence intervals to some – but not all – of these estimates. We have implemented our new methodolgy in the form of S-PLUS functions. We have used these functions to demonstrate the usefulness of this methodolgy for studying the time-varying properties of an aerothermal time series provided to us by our sponsors. Our phase I research has thus established the foundation for our phase II efforts, in which we will

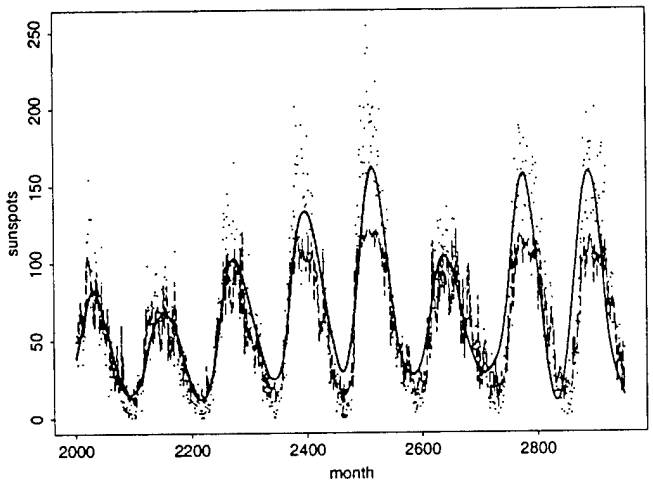


Figure 16: Prediction results the sunspots data (dots) using LLWS prediction on selected wavelet subbands (solid thick lines) and nearest neighbor prediction on the original series (solid thin lines).

extend the methodology to make it applicable to a wider range of problems and create a library of commerical-grade C routines.

Our phase II research will extend the phase I research by completing the statistical theory behind our wavelet-based estimators. In phase II we will also improve the computational efficiency, robustness and portability of our computer code by rewriting our algorithms as C routines. In addition we will create code for a much wider collection of algorithms that can be of use in modelling fractal processes. We will also provide our Air Force sponsors with code in whatever form they deem best to allow them to make use of our research results in their own work (most likely either in the form of a C library or as a MATLAB toolbox with an appropriate GUI to help guide the non-expert analyst on the use of the methodology).

The phase II research will lay the groundwork for the development of commercial-grade software toolkits in both S-PLUS and MATHCAD for wavelet-based analysis of time series exhibiting fractal properties. In addition, the training course that we develop on analyzing non-stationary multi-scale fractal processes can be turned into documentation suitable for use with these toolbox.

## 6.2 Commercial Potential

A primary strength of this proposal is a realistic and credible commercial plan. The heart of the plan is develop state-of-the-art software products which will appeal to a broad audience of users. MathSoft is a market leader in wavelet and advanced statistical technology. MathSoft also has an impressive record on commercialization of Government funded research.

Here we present our specific commercialization plans (section 6.2.1), give background on our company (section 6.3) and its past record of commercializing government-sponsored research (section 6.4).

### 6.2.1 Specific Commercialization Plans

Our research will lead to phase III development of a user-friendly S-PLUS and MATHCAD toolboxes for analysis of fractal processes, a library of portable and reusable software tools, and short courses with an associated book/hypermedia document that will guide practitioners in the analysis of multi-scale fractal processes. In commercialization of the fractal processes toolkits, we will be guided by our experience in developing and marketing wavelets technology, which resulted in the S+WAVELETS module for S-PLUS, a MATHCAD Wavelets extension pack, a book published by Springer–Verlag, educational courses taught to industry and research laboratories, and consulting opportunities in industry (e.g., cellular telephone fraud detection). Because the underlying software will be based on a well organized set of C libraries, we will be able to incorporate these tools into more than one product. Marketing the toolkits on more than one platform is critical for successful commercialization since the toolkits individually target relatively small markets.

Our specific commercialization plans, roughly in order of priority, are as follows.

**S-Plus Fractal Processes Toolbox:** The primary development that will follow in phase III from the proposed research will be a toolkit based on the collection of C routines developed in phase II. We will embed this toolkit within S-PLUS as a module for advanced fractal analysis. S-PLUS is an ideal platform for the proposed development, with a huge existing customer base including technically literate data analysts from a variety of disciplines.
**Fractal Processes Extension Pack:** A second product which would naturally evolve from our research plans is a Fractal Processes extension pack for MATHCADA MATHCAD extension pack would have a lower price point than an S-PLUS toolbox and would leverage the large installed base of MATHCAD (currently over 1 million users).
**Books and Hypermedia:** A key component to commercial success of our research will be the development of a book linking the practice and theory of fractal processes analysis. With the advent of multimedia technology and the World Wide Web, we can go beyond the traditional textbook format and provide a state-of-the-art interactive hypermedia book linked to the Fractal Processes Toolbox. The book will contain a rich collection of applications drawn from our phase II and other research efforts. We will also pursue more traditional outlets for publication.
**Other Vertical Markets:** Full realization of our research goals will make analysis of fractal processes a standard part of signal processing. We see substantial opportunity to license our technology to specialized software systems dedicated to vertical markets where fractal signals are important, including biomedical engineering and finance. In addition, if we embed our C library within a MATLAB toolbox to meet the requirements of our sponsors, we will seek avenues for marketing this toolkit.
**Teaching and Consulting:** To supplement the software products and books, we expect to offer related short courses and software training. Short courses in signal processing oriented towards industry and government are routinely offered by various groups. A large part of the Data Analysis Products Division's revenues results from training classes. The tuition for training classes and short courses typically exceeds $1,000 per participant. Our software and casebook will also serve as a magnet for recruiting consulting projects. The Data Analysis Products Division is rapidly expanding its consulting group, partly as a result of its high-end research efforts (e.g., in wavelet analysis). We will aggressively pursue related consulting, particularly in areas such as financial engineering.

## 6.3 Proposing Company, Mission and Main Products

The research and software development for this project will be done primarily at the facilities of the Data Analysis Products Division of MathSoft, Inc. MathSoft is a U.S. owned publicly traded small business (NASDAQ: MATH) that is based in Cambridge, Massachusetts, and specializes in mathematically oriented software. The Data Analysis Products Division (DAPD) specializes in statistical software products and includes the Research Department. Overall the company has 195 employees, with 95 of these being in the DAPD.

The Research Department has over 36 employees of whom approximately 28 have Ph.D.'s in disciplines such as statistics, electrical engineering, mechanical engineering, physics, computer science and applied mathematics. Research staff actively collaborate with researchers at universities and other institutions. These connections are particularly strong with the University of Washington.

The primary mission of the DAPD is to develop, market, and support cutting edge scientific computing software environments for high-interaction statistical and visual data analysis. The DAPD offers the S-PLUS and AXUM product line. S-PLUS is an interactive computing environment for graphics, data analysis, statistics and mathematical computing. S-PLUS is a super-set of the S object-oriented language and system designed by R. Becker, J. Chambers and A. Wilks at AT&T Bell Laboratories, Murray Hill, NJ, for which Chambers won the prestigious 1998 ACM Software System Award (this annual award carries a prize of $10,000 and has been given in the past to the developers of, e.g., UNIX, TeX, PostScript, TCP/IP and the World Wide Web). The DAPD recently released S-PLUS 4.0, incorporating advanced, object-oriented graphics into the S-PLUS environment. S-PLUS 4.0 was recently given the Personal Computer World Editor's Choice Award. Our customer base represents almost every major industry, with particular strength in high-tech manufacturing, biotechnology, engineering, and finance. S-PLUS is available in UNIX and Windows versions. Our product STATSERVER supports distributed access to S-PLUS over internal and external networks. Web browsers and customized applications can submit S-PLUS expressions to a STATSERVER and retrieve the results, including graphics. STATSERVER 2.0 recently won a prestigious industry award, when it was named to the Crossroads A-list by Open Systems Advisors.

The flagship product of MathSoft is MATHCAD, a numeric and symbolic mathematical analysis software package. MATHCAD combines natural notation equation manipulation, text and graphics into a single electronic document. MathSoft is also a strong played in the education market with its award-winning STUDYWORKS! software for building skills in mathematics and science for high school students. The company has more than one million users of its MATHCAD, STUDYWORKS!, S-PLUS, STATSERVER and AXUM software worldwide. Users include technical professionals

worldwide at more than 90% of the Fortune 1,000 companies and over 500 government installations, and students and faculty at over 2,000 colleges and universities.

### 6.4 Commercialization Record

The Data Analysis Products Division of MathSoft has an outstanding record in the commercialization of advanced data analysis technology. Our core product, S-PLUS, is a commercial version of the S language developed in the research environment of Lucent technologies. In fact, the DAPD would never have existed if it were not for our abilities to commercialize data analysis software.

The DAPD has further established a record of commercializing advanced data analysis software developed partially using government funds under the SBIR program and the NASA EOCAP program. In the past four years, we have completed eight Phase II SBIR awards and one NASA EOCAP award. Partially supported by these awards, we have commercialized and shipped six products: S+WAVELETS, S+API, S+DOX, S-PLUS for ARC/INFO, S+SPATIAL, and S-PLUS for ArcView GIS. Additional products are under development based on SBIR-funded work in signal and image processing, group sequential analysis, and statistics for data with missing values. In addition, we have shipped a MATHCAD Wavelets function pack in 1998 based on technology developed for S+WAVELETS.

## 7 Summary

Each of the objectives in Sec. 3 has been addressed in our research efforts for phase I. The feasibility of this project is estimated to be very high considering (i) the large number of functions written for the existing S+WAVELETS module, (ii) the promising results of these functions as applied to real aerothermal turbulence data, (iii) the commercialization record of MathSoft, Inc. and (iv) the demand for such tools in other areas such as in cardiodynamics, (internet) traffic modeling, and financial time series analysis to name a few. Through partial funding by this STTR phase I contract, our research has lead to (2) technical reports, (1) conference paper, (2) journal articles (pending acceptance), and (1) book on wavelet methods for time series analysis.

We would like to thank our sponsors for funding this project and we look forward to our cooperative phase II effort.

# References


[1] N. Aubry, P. Holmes, J.L. Lumley, and E. Stone. The dynamics of coherent structures in the wall region of a turbulent boundary layer. *Journal of Fluid Mechanics*, 192:115–173, 1988.

[2] J.B. Bassingthwaighte, L.S. Liebovitch, and B.J. West. *Fractal Physiology.* Oxford University Press, New York, 1994.

[3] H.H. Bau and K.E. Torrance. On the stability and flow reversal of an asymmetrically heated open convection loop. *Journal of Fluid Mechanics*, 106:412–433, 1981.

[4] J. Beran. *Statistics for Long-Memory Processes.* Chapman & Hall, New York, 1994.

[5] T. Bollerslev. Generalized autoregressive conditional heteroskedasticity. *Journal of Econometrics*, 31:307–327, 1986.

[6] P. Craigmile, D.B. Percival, and P. Guttorp. The impact of wavelet coefficient correlations on fractionally differenced processes. In *Proceedings of the Third European Conference of Mathematics*, Barcelona, Spain, 2000. Birkhauser Verlag.

[7] P. Craigmile, D.B. Percival, and P. Guttorp. Trend assessment using the discrete wavelet transform. Technical report, University of Washington, Department of Statistics, 2000.

[8] P. Craigmile, D.B. Percival, and P. Guttorp. Wavelet-based parameter estimation for trend contaminated fractionally differenced processes. *Journal of Time Series Analysis*, 2000. submitted for review.

[9] I. Daubechies. *Ten Lectures on Wavelets.* SIAM, Philadelphia, 1992. Number 61 in CBMS-NSF Series in Applied Mathematics.

[10] C. W. J. Granger and R. Joyeux. An introduction to long-memory time series models and fractional differencing. *Journal of Time Series Analysis*, 1:15–29, 1980.

[11] J. R. M. Hosking. Fractional differencing. *Biometrika*, 68:165–176, 1981.

[12] R. Keolian, L. A. Turkevich, S. J. Putterman, I. Rudnick, and J. A. Rudnick. Subharmonic sequences in the faraday experiment: Departures from period doubling. *Physical Review Letters*, 47(16):1133–1151, 1981.

[13] Z. Q. Lu and R. L. Smith. Estimating local lyapunov exponents. In C. Cutler and D. Kaplan, editors, *Nonlinear Dynamics and Time Series: A Bridge Between the Physical and Statistical Sciences*, pages 135–151. American Mathematical Society, Fields Institute Communications, 1997.

[14] Z.Q. Lu. Predicting nonlinear time series. *Proceedings of American Statistical Association*, 1996. Business and Economics Section.

[15] Z.Q. Lu. Nonparametric regression with singular design. *Journal of Multivariate Analysis*, 70:177–201, 1999.

[16] Z.Q. Lu. Statistical estimation of local lyapunov exponents: Toward characterizing predictability in nonlinear systems. Under revision for the Journal of American Statistical Association, 2000.

[17] Z.Q. Lu and L.M. Berliner. Markov switching time series models with application to a daily runoff series. *Water Resources Research*, 35(2):523–534, 1999.

[18] S. Mallat. A theory for multiresolution signal decomposition: The wavelet representation. *IEEE Transactions on Pattern Analysis and Machine Intelligence*, 2(7):674–93, 1989.

[19] F.C. Moon. *Chaotic and Fractal Dynamics: An Introduction for Applied Scientists and Engineers.* John Wiley and Sons, Inc, New York, NY, 1992.

[20] G. S. Papanicolaou, K. Solna, and D. Washburn. Segmentation independent estimates of turbulence parameters. In *SPIE Proceedings, Airborne Laser Advanced Technology*, volume 3381, pages 256–267, Orlando, FL, April 1998.

[21] D. B. Percival and P. Guttorp. Long-memory processes, the Allan variance and wavelets. In E. Foufoula-Georgiou and P. Kumar, editors, *Wavelets in Geophysics.* Academic Press, Inc., New York, 1994.

[22] D.B. Percival and A. Walden. *Wavelet Methods for Time Series Analysis.* Cambridge University Press, Cambridge, UK, 2000.

[23] P. L. Read, M. J. Bell, D. W. Johnson, and R. M. Small. Quasi-periodic and chaotic flow regimes in a thermally driven, rotating fluid annulus. *Journal of Fluid Mechanics*, 238:599–632, 1992.

[24] H.L. Swinney. Observations of order and chaos in nonlinear systems. *Physica D*, 7:3–15, 1983.